Available online at www.sciencedirect.com

ScienceDirect

Procedia Engineering 10 (2011) 3540–3545

Engineering Procedia

ICM11

Effects of manufacturing-induced residual stresses and strains on hydrogen embrittlement of cold drawn steels

J. Toribio[a*], M. Lorenzo[b], D. Vergara[a], V. Kharin[a]

[a]*Department of Materials Engineering, University of Salamanca E.P.S., Campus Viriato, Avda. Requejo 33, 49022 Zamora, Spain*
[b]*Department of Mechanical Engineering, University of Salamanca*
E.T.S.I.I., Avda. Fernando Ballesteros 2, 37700 Béjar, Spain

Abstract

Cold drawn wires of eutectoid pearlitic steel are widely used for prestressing concrete structures that usually work in harsh environments, so that stress corrosion cracking of prestressing steel is a problem of major technological concern. In this paper a previous model developed by the authors is applied to analyse the influence of the residual stress-and-strain profiles after cold drawing on the hydrogen embrittlement susceptibility of prestressing steel wires. Numerical results show the relevant role of both residual stress and strain field in hydrogen diffusion in this material.

Keywords: Prestressing steel, cold drawing, residual stresses, residual strains, hydrogen diffusion, numerical modelling;

1. Introduction

The effects of cold drawing on pearlitic steels wires make them suitable for a broad range of high performance applications in engineering. Briefly, at the macroscopic level, the consequences of cold drawing are, namely, a noticeable increment of the wire resistance and a clear improvement of material toughness. These improvements of mechanical properties of the cold drawn steel are caused by microstructural changes [1-2] during cold drawing (reduction of interlamellae spacing, slenderising of pearlitic colonies and progressive orientation of both pearlite colonies and lamellae). However a non-uniform distribution of plastic strain after cold drawing is the origin of an undesired effect of manufacturing: the appearance of a distribution of residual stresses at the end of the process [3].

The residual stresses and plastic strains generated after cold drawing process are not negligible [3] and consequently these states should be taken into account to achieve a better approach to the real mechanical

behavior of prestressing steel wires in service conditions. Thus, the determination of those states is a key issue in the analysis of diverse phenomena related with in-service performance such as fatigue cracking [4] or hydrogen embrittlement (HE) [5,6], prestressing steels being particularly susceptible to this type of fracture phenomenon [7].

In scientific literature, the quantitative analysis of the influence of residual stresses on HE in pearlitic steel appeared in 1991 in the pioneering work [5] where the role of residual stresses in HE was originally revealed by means of a finite element simulation considering theoretical residual stress distributions along wire radius. The earlier model was enhanced in [6] where the influence of real residual stresses and strains generated by a one-step drawing on HE of pearlitic steel wires was analyzed, establishing the key role that plastic strain plays in hydrogen diffusion processes. To reveal the importance of drawing conditions, the former study was enlarged performing an analysis of the influence of two different drawing reductions on the HE [8]. Within this framework, the present study is established as a new step in the research line established in previous works, the aim of this paper being the analysis of the influence of residual stresses and strains states after a real industrial cold drawing process (the whole manufacturing chain in six stages of cold drawing) on the HE susceptibility of commercial prestressing steel wire after a progressive (multi-step) cold drawing process.

2. Residual stresses and plastic strains due to progressive cold drawing

In this work, a real (commercial) cold drawing process in several passes (i steps or stages) was modelled. The base material at the beginning of the manufacturing chain was a hot-rolled pearlitic steel (0.740% C, 0.700% Mn, 0.200% Si, 0.015% P, 0.023% S) which Young modulus and 0.2%-offset yield strength are E = 199 GPa and σ_Y = 710 MPa respectively. With them, to perform the finite-element mechanical simulations of stress and strain fields, $\underline{\underline{\sigma}}(\boldsymbol{r})$ and $\underline{\underline{\varepsilon}}(\boldsymbol{r})$, the constitutive model was chosen to be an elastoplastic solid with von Mises yield surface, associated flow rule, and isotropic strain-hardening.

Cold drawing consists of the pass of the steel wire through a hard die (Fig. 1). The die was modelled with an inlet angle $\alpha = 7^{\circ}$, and the material of the die (tungsten carbide) was considered to be rigid due to its very high Young modulus in relation to that of the wire. Friction between the wire and the die was not considered in the numerical modelling. Initial dimensions of the wire were d_0 = 12 mm (initial diameter) and L_0 = 60 mm (initial length). The commercial cold-drawn pearlitic wire used in this analysis was obtained after six passes (cf. diameter reduction from d_0 =12 mm to d_6=7mm).

The axisymmetric formulation is suitable for simulations. Corresponding finite element model was created to model the drawing process in cylindrical coordinates (r,z) shown in Fig. 1. The boundary condition of the prescribed axial displacement was imposed on the front extreme of the rod. Elastoplastic large deformation – large strain calculations were performed using a general-purpose finite element code with updated lagrangian formulation. Several finite element meshes formed by four-node quadrilaterals were tried till the acceptable mesh-convergence of the result was ensured.

Computer modelling allowed a better knowledge of the evolutions of stress-strain states during the cold drawing process and especially of the final distributions of *residual* hydrostatic stress σ and equivalent plastic strain $\bar{\varepsilon}_P$ in the commercial prestressing steel wire (σ and $\bar{\varepsilon}_P$ are the key variables in the matter of HE susceptibility of prestressing steels [6]). Following sections of the paper offer the distributions of both hydrostatic stress σ, equivalent plastic strain $\bar{\varepsilon}_P$ obtained from the mechanical modelling (stress-strain finite element analysis: first computation). Such stress-strain distributions are used later as input data in the diffusion modelling (stress-*and*-strain assisted diffusion of hydrogen: second computation) to obtain the hydrogen concentration evolution with time at any point of the prestressing steel wire.

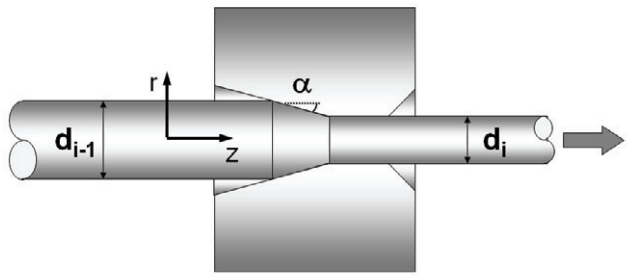

Fig. 1. Scheme of one pass of the cold drawing process.

3. Stress and strain fields in the cold drawn steel wire

Fig. 2 shows the evolution of hydrostatic stress during the initial (hot rolled bar) and final (prestressing steel wire) stages of cold drawing as a function of the radial coordinate (r). It is seen in Fig. 2a that the level of *residual* hydrostatic stress increases and the diameter decreases progressively with cold drawing preocess. Compressions ranging between –550 MPa and –900 MPa are always obtained in the wire core (central position r=0), whereas tensions ranging between +550 MPa and +650 MPa are achieved near the wire surface. This is a very dangerous situation, since the pioneering paper [5] undoubtedly demonstrates by *quantitative* modelling the deleterious effect of near-surface tensile residual stresses on the HE performance of cold-drawn prestressing steel wires.

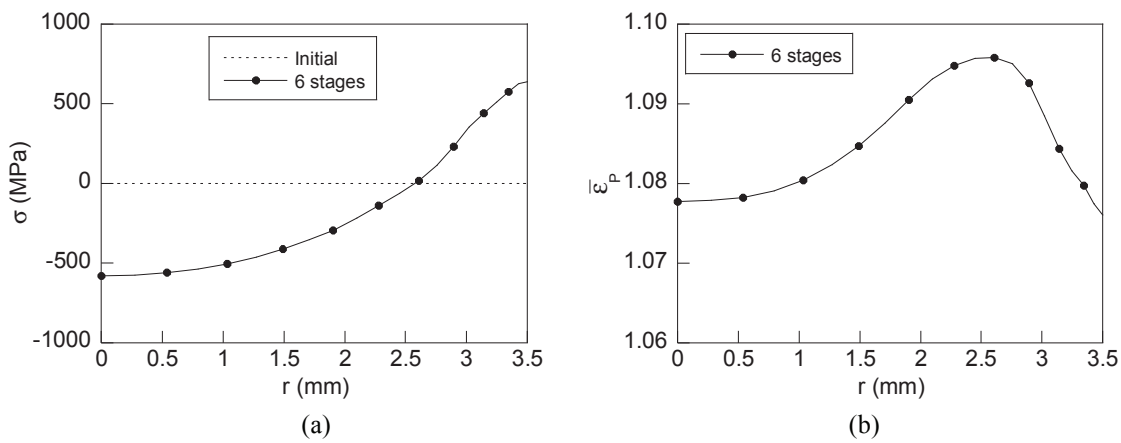

Fig. 2. Evolution of (a) hydrostatic stress and (b) equivalent plastic strain after cold drawing.

Fig. 2b shows the evolution with cold drawing of the equivalent plastic strain $\bar{\varepsilon}_P$ affecting the strain-dependent component of the solubility. Thus, this figure offers the distributions (as a function of the radial coordinate (r)) of equivalent plastic strain after each cold drawing pass, and this variable $\bar{\varepsilon}_P$ could be properly called residual plastic strain.

4. Hydrogen distribution in the cold drawn steel wire

To discriminate the contributions of stress and plastic strain on hydrogenation of wire, three hydrogen diffusion schemes were considered: (a) *stress-and-strain* assisted diffusion, according to equation (1a); (b) stress-only assisted diffusion, according to equation (1b) with $\nabla K_S(\bar{\varepsilon}_P) = 0$; (c) conventional diffusion with no stress assistance (equation 1c). The respective equations are:

$$\mathbf{J} = -D(\bar{\varepsilon}_p)\left\{\nabla C - C\left[\frac{V_H}{RT}\nabla\sigma + \frac{\nabla K_{S\varepsilon}(\bar{\varepsilon}_p)}{K_{S\varepsilon}(\bar{\varepsilon}_p)}\right]\right\}, \tag{1a}$$

$$\mathbf{J} = -D\{\nabla C - C\Omega\nabla\sigma\}, \tag{1b}$$

$$\mathbf{J} = -D\nabla C\,. \tag{1c}$$

where $K_{S\varepsilon}$ is the strain-dependent component of solubility was obtained from next equation [9]:

$$K_{SM}^{(i)}(r) = 1 + 4\bar{\varepsilon}_P^{(i)}(r) \tag{2}$$

Model parameters were chosen as follows: temperature T = 323 K; partial molar volume of hydrogen for iron-based alloys, V_H = 2 cm^3/mol [10]; hydrogen diffusivity may be as low as 10^{-12} m^2/s and less for heavily cold drawn pearlitic steels [5]. The results of the computations for the three models considered (equations 1a-1c) applied to the prestressing steel wire (after 6 stages) are presented as hydrogen concentration distributions in Fig. 3 (spatial distributions against the dimensionless radial coordinate r/a, a being the outer wire radius) in terms of dimensionless concentration $C(r,t)/C^*$ where the reference concentration C^* represents the hydrogenating capacity of environment modified by applied stress σ_{app}, i.e., the equilibrium hydrogen concentration in stressed virgin material, which within elasticity limits is $C^* = C_{eq}^0 K_{S\varepsilon}(\bar{\varepsilon}_P)\exp(\Omega\sigma_{app}/3)$.

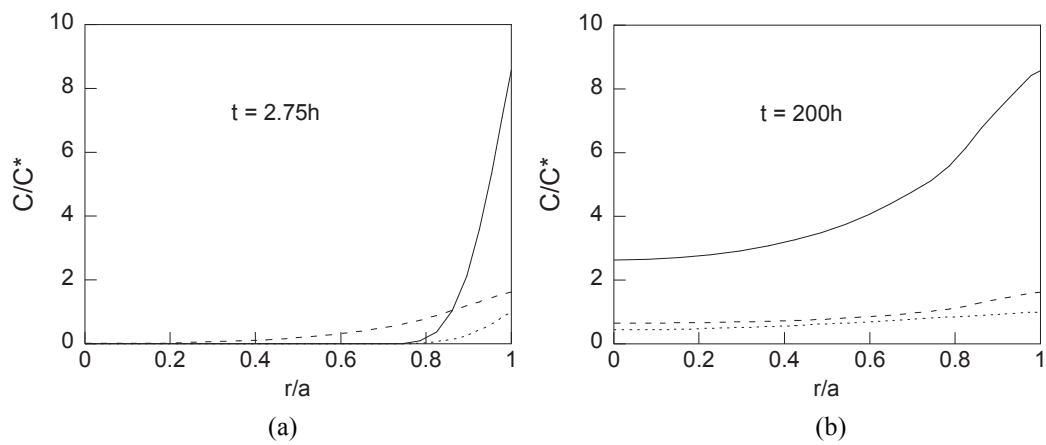

Fig. 3. Distributions of relative concentrations of hydrogen (C/C*) as a function of the dimensionless radial coordinate *r/a*, at two different diffusion times, 2.75 hours (a) and 200 hours (b), for the three modelling schemes: stress-and-strain assisted diffusion (full line), stress-only assisted diffusion (dashed line) and conventional diffusion with no stress or strain assistance (dotted line).

Results show that the effects of residual stress and strain on hydrogenation consist in a *local* increase of hydrogen concentration in the highly stresses areas of the wire, i.e., near the wire surface where hydrostatic residual stresses are tensile and plastic strains are high enough after the whole drawing process. This is clearly observed in Fig. 3 where the concentration distributions at the wire skin (i.e. at $r/a = 1$) and its vicinity, especially for short diffusion times (Fig. 3a) for which there is no time to supply hydrogen to more internal areas. These numerical results confirm the danger of tensile residual stresses near the wire surface in the matter of HE susceptibility of prestressing steels.

With regard to the distinction between stress-only and stress-strain assisted hydrogenation, two competing effects of the stress and plastic strain fields on hydrogen diffusion appear when *both* the stress and the strain fields are considered. The first one is the increase of hydrogen solubility due to tensile stresses and accumulated plastic strain, which results in rising hydrogen absorption by a metal. On the other hand, the decrease of hydrogen diffusivity (of its mobility) in plastically strained material, slows-down this process of enhanced hydrogen accumulation in the wires.

To analyze the two afore-said effects, Fig. 3 is the key item. It shows that relative over-hydrogenation occurs at the wire surface $r = a$ and its vicinity (critical area where a hydrogen–induced crack could appear). In terms of the hydrogenation of a wire skin, where critical events of HE can be expected to occur (cf., [5]), residual strain field dramatically increases the amount of hydrogen accumulated in this skin at short diffusion times ($t = 2.75$ h; Fig. 3a), and increases *even more* this amount at long exposure times ($t = 200$h; Fig. 3b), thus enhancing the hydrogenation of prestressing steel wires. Therefore, in highly strained materials as cold drawn steels *the increase of hydrogen solubility due to accumulated plastic strain predominates over the decrease of hydrogen diffusivity (mobility) in plastically strained material*.

The stress-strain assisted diffusion equation predicts a much higher amount of hydrogen in the critical area (near to wire surface [5]) than the stress-only assisted diffusion or the conventional diffusion models. Therefore, *plastic strain fields must be taken into account in hydrogen diffusion equations in cold drawn wires because the consideration of stress-only assisted diffusion leads to dramatic underestimation of the hydrogen content in the critical region*.

5. Conclusions

(i) Residual stress distributions are of tensile nature in the wire skin and its vicinity, with a maximum just at the surface. This is very dangerous from the point of view of the HE susceptibility of the cold drawn wires, considering the deleterious effect of such tensile near-surface residual stresses on the performance of the prestressing steel wires, since tensile stresses are driving forces for hydrogen entry and diffusion.

(ii) There is a progressive accumulation of equivalent plastic strain with cold drawing, and this can affect hydrogen diffusion assisted by stress and strain in two ways: firstly, by rising hydrogen solubility due to accumulated plastic strain, thereby resulting in rising hydrogen absorption; secondly, by lowering hydrogen diffusivity (and thus mobility) in plastically strained material, thus delaying hydrogen accumulation in the wires.

(iii) The maximum values of hydrogen concentration are achieved at the wire skin and its vicinity. This is valid for both short and long times for diffusion, although in the case of long exposures to hydrogen the penetration distances are higher.

(iv) Plastic strain fields must be taken into account in hydrogen diffusion equations in cold drawn wires because the consideration of stress-only assisted diffusion leads to dramatic underestimation of the hydrogen content in the critical region.

Acknowledgements

This research was supported by MCYT (Grant MAT2002-01831), MEC (Grant BIA2005-08965), MCINN (Grant BIA2008-06810) and JCyL (Grants SA067A05, SA111A07 y SA039A08). The steel used in the experimental programme was provided by EMESA TREFILERÍA (La Coruña, Spain).

References

[1] Toribio J, Ovejero E. Microstructure evolution in a pearlitic steel subjected to progressive plastic deformation. *Mater Sci Eng* 1997;**A234–236**:579–82.

[2] Zelin M. Microstructure evolution in pearlitic steels during wire drawing. *Acta Mater* 2002;**50**:4431–47.

[3] He S, Van Bael A, Li SY, Van Houtte P, Mei F, Sarban A. Residual stress determination in cold drawn steel wire by FEM simulation and X-ray diffraction. *Mater Sci Eng* 2003;**A346**:101–7.

[4] Webster GA, Ezeilo AN. Residual stress distributions and their influence on fatigue lifetimes. *Inter J Fat* 2001;**23**:S375–83.

[5] Toribio J, Elices M. Influence of residual stresses on hydrogen embrittlement susceptibility of prestressing steels. *Int J Solids Struct* 1991;**28**:791–803.

[6] Toribio J, Kharin V, Vergara D, Blanco JA, Ballesteros JG. Influence of residual stress and strains generated by cold drawing on hydrogen embrittlement of prestressing steels. *Corros Sci* 2007;**49**:3557–69.

[7] Perrin M, Gaillet L, Tessier C, Idrissi H. Hydrogen embrittlement of prestressing cables. *Corros Sci* 2010;**52**:1915–26.

[8] Toribio J, Lorenzo M, Vergara D, Kharin V. Hydrogen degradation of cold drawn wires: a numerical analysis of drawing-induced residual stresses and strains. *Corros* 2011;*In press*.

[9] Astiz MS, Álvarez JA, Gutiérrez-Solana F. Modelo numérico para analizar el efecto del hidrógeno sobre los procesos de fisuración dúctil. *Anal Mecá Fract* 1998;**15**:79–84.

[10] Hirth JP. Effects of hydrogen on the properties of iron and steel. *Metall. Trans* 1980;**A11**:861–90.